Supporting Information for

Conjugated Microporous Copolymer Networks with Enhanced Gas Adsorption

Miao Yu, Xiaoyan Wang, Xiao Yang, Yang Zhao, Jia-Xing Jiang*

School of Materials Science and Engineering, Shaanxi Normal University, Xi'an, 710062, Shaanxi, P. R. China

E-mail: jiaxing@snnu.edu.cn

Experimental section

Synthesis of CP-CMP2: DBA (331.5 mg, 2.0 mmol), TBrPy (414.4 mg, 0.8 mmol) and TBrCz (96.6 mg, 0.2 mmol) were used in this polymerization (yield: 83.6%), details as discribed for **CP-CMP1**. Elemental combustion analysis (%) Calcd for $(C_{27.2}H_{13.8}N_{0.2})_n$: C 95.16; H 4.02; N 0.82; Found: C 85.08; H 4.25; N 0.88.

Synthesis of CP-CMP3: BDA (331.5 mg, 2.0 mmol), TBrPy (310.8 mg, 0.6 mmol) and TBrCz (193.2 mg, 0.4 mmol) were used in this polymerization (yield: 82.5%). Elemental combustion analysis (%) Calcd for $(C_{26.4}H_{13.6}N_{0.4})_n$: C 94.29; H 4.05; N 1.66; Found: C 83.48; H 4.21; N 1.69.

Synthesis of CP-CMP4: BDA (331.5 mg, 2.0 mmol), TBrPy (259 mg, 0.5 mmol) and TBrCz (241.5 mg, 0.5 mmol) were used in this polymerization (yield: 82.7%). Elemental combustion analysis (%) Calcd for $(C_{26}H_{13.5}N_{0.5})_n$: C 93.83; H 4.06; N 2.11; Found: C 82.37; H 4.09; N 1.93.

Synthesis of CP-CMP5: BDA (331.5 mg, 2.0 mmol), TBrPy (207.2 mg, 0.4 mmol) and TBrCz (289.8 mg, 0.6 mmol) were used in this polymerization (yield: 86.9%). Elemental combustion analysis (%) Calcd for $(C_{25.6}H_{13.4}N_{0.6})_n$: C 93.37; H 4.07; N

2.56; Found: C 81.94; H 4.24; N 2.39.

Synthesis of CP-CMP6: BDA (331.5 mg, 2.0 mmol), TBrPy (103.6 mg, 0.2 mmol) and TBrCz (386.4 mg, 0.8 mmol) were used in this polymerization (yield: 80.3%). Elemental combustion analysis (%) Calcd for $(C_{24.8}H_{13.2}N_{0.8})_n$: C 92.42; H 4.10; N 3.48; Found: C 80.11; H 4.33; N 3.06.

Synthesis of CP-CMP7: BDA (331.5 mg, 2.0 mmol) and TBrCz (483 mg, 1.0 mmol) were used in this polymerization (yield: 85.1%). Elemental combustion analysis (%) Calcd for $(C_{24}H_{13}N)_n$: C 91.4, H 4.15, N 4.44; Found: C 77.81; H 4.56; N 3.45.

Table S1. Surface areas for the copolymer networks from different batch

Copolymer	1st batch		2nd batch		3rd batch		SD_{BET} [c]	SD_{Micro} [d]
	S_{BET} [a] [$m^2 g^{-1}$]	S_{Micro} [b] [$m^2 g^{-1}$]	S_{BET} [a] [$m^2 g^{-1}$]	S_{Micro} [b] [$m^2 g^{-1}$]	S_{BET} [a] [$m^2 g^{-1}$]	S_{Micro} [b] [$m^2 g^{-1}$]	n=3	n=3
CP-CMP1	1191	801	1079	805	1091	754	50 (4.5%)	23 (2.9%)
CP-CMP2	1067	796	972	699	998	785	40 (3.9%)	43 (5.6%)
CP-CMP3	883	632	964	739	904	627	34 (3.7%)	52 (7.8%)
CP-CMP4	1083	754	960	666	1039	759	51 (4.9%)	43 (5.9%)
CP-CMP5	2241	1129	2142	1023	2086	1016	64 (2.9%)	52 (4.9%)
CP-CMP6	1764	909	1824	933	1694	889	53 (3.0%)	21 (2.3%)
CP-CMP7	847	699	893	702	904	666	25 (2.8%)	16 (2.3%)

[a] BET Surface area calculated from N_2 adsorption isotherm in the relative pressure (*P/Po*) range from 0.05 to 0.20 using the Brunauer–Emmett–Teller method, [b] Micropore surface area calculated from the N_2 adsorption isotherm using t-plot method based on the Harkins-Jura Equation, [c] Standard deviation of BET surface area, [d] Standard deviation of micropore surface area (the number in parentheses is relative standard deviation).

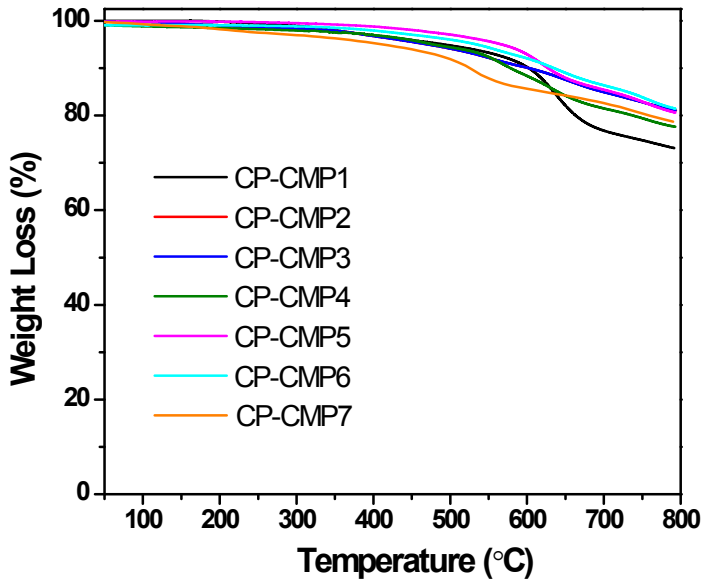

Figure S1. Thermogravimetric analysis trace of the copolymer networks under a nitrogen atmosphere with a heating rate of 10 °C/min.

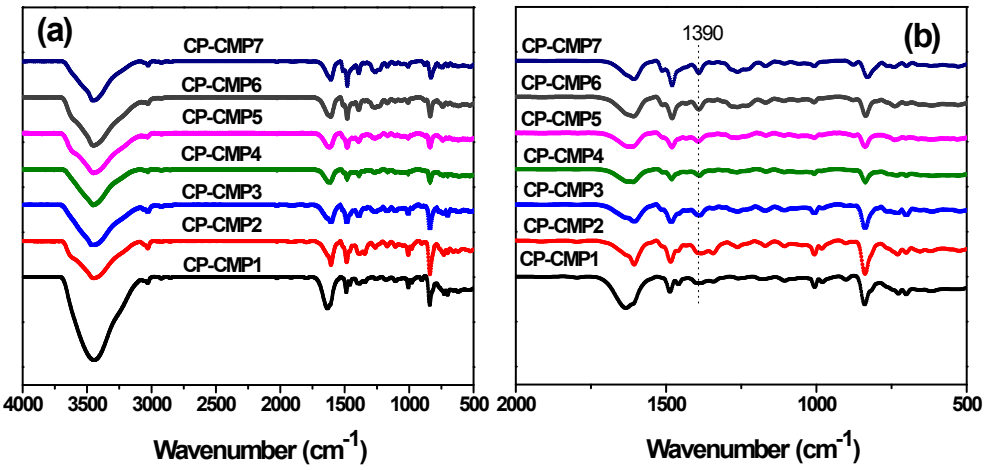

Figure S2. FT-IR spectra for the copolymer networks.

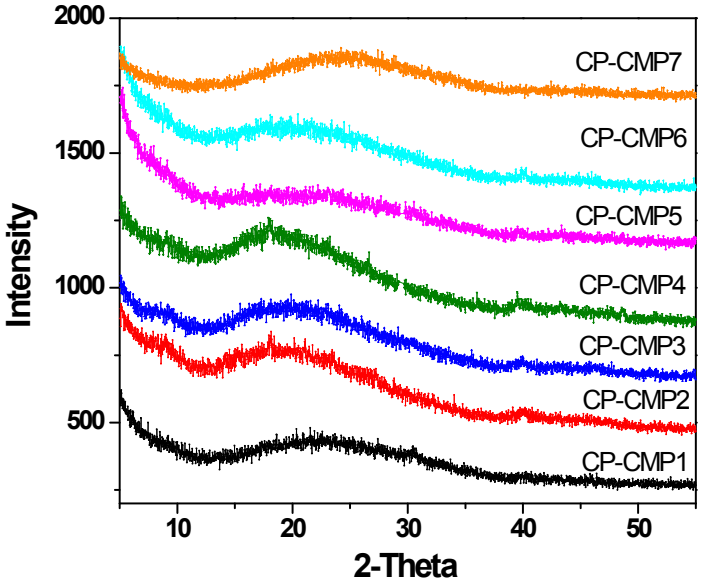

Figure S3. Powder XRD patterns of the copolymer networks.

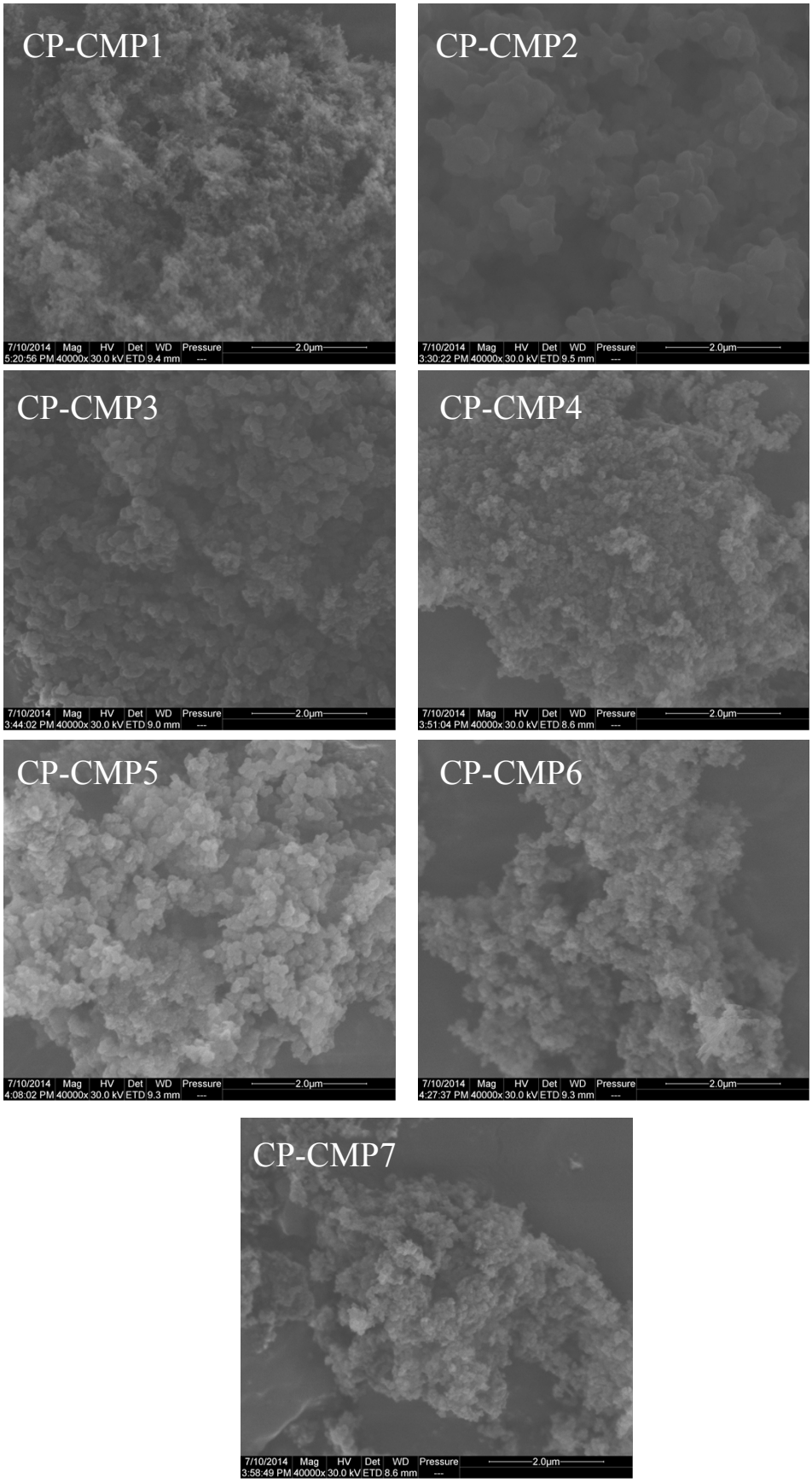

Figure S4. Scanning electron microscopy images of the copolymer networks with a scale bar of 2.0 µm.

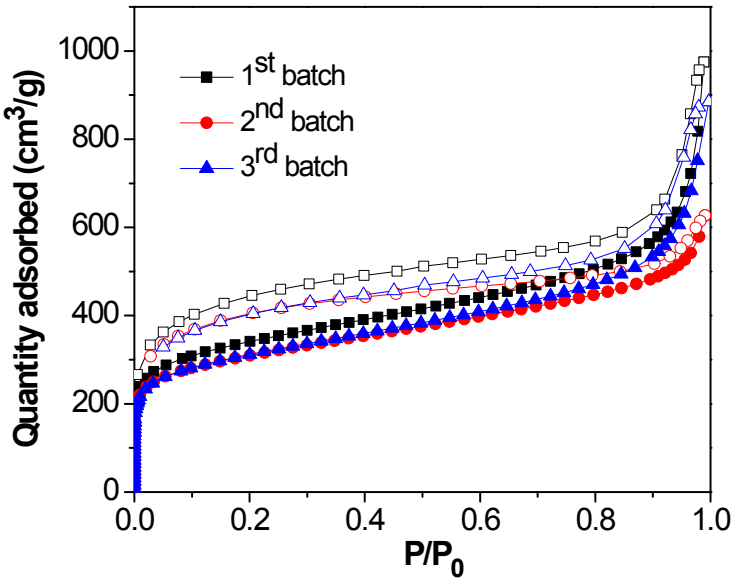

Figure S5. Nitrogen adsorption (filled symbols) and desorption (open symbols) isotherms for CP-CMP1 produced from different batch.

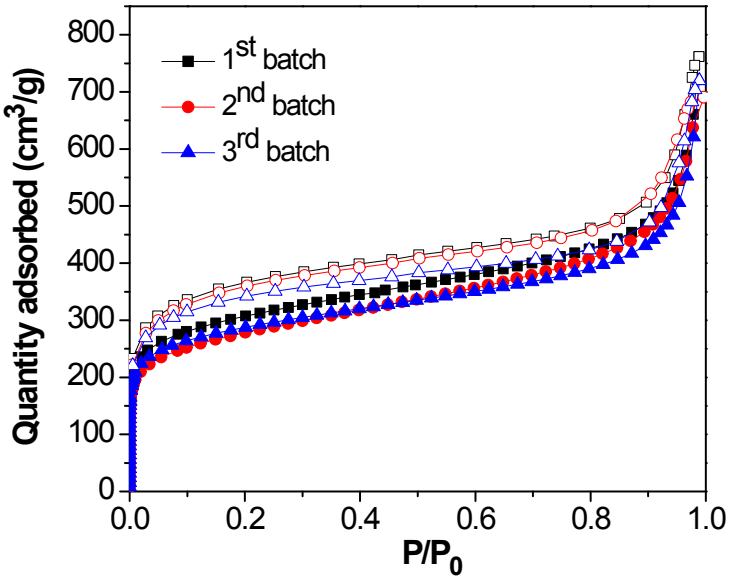

Figure S6. Nitrogen adsorption (filled symbols) and desorption (open symbols) isotherms for CP-CMP2 produced from different batch.

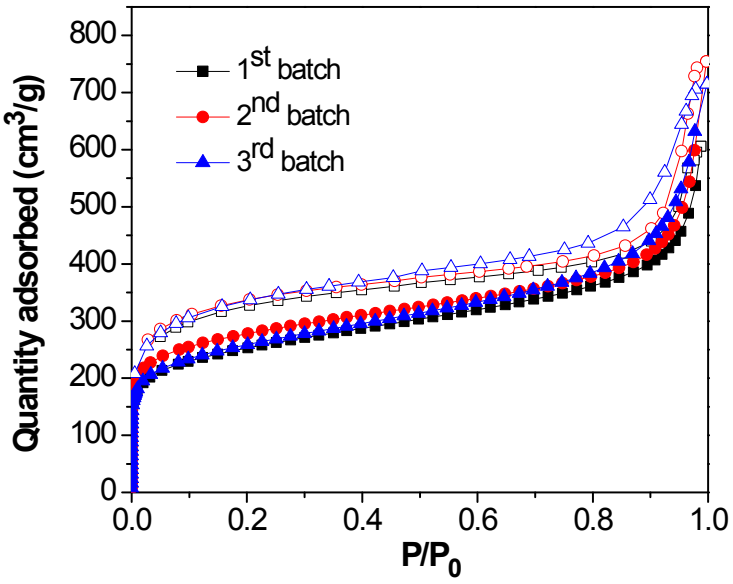

Figure S7. Nitrogen adsorption (filled symbols) and desorption (open symbols) isotherms for CP-CMP3 produced from different batch.

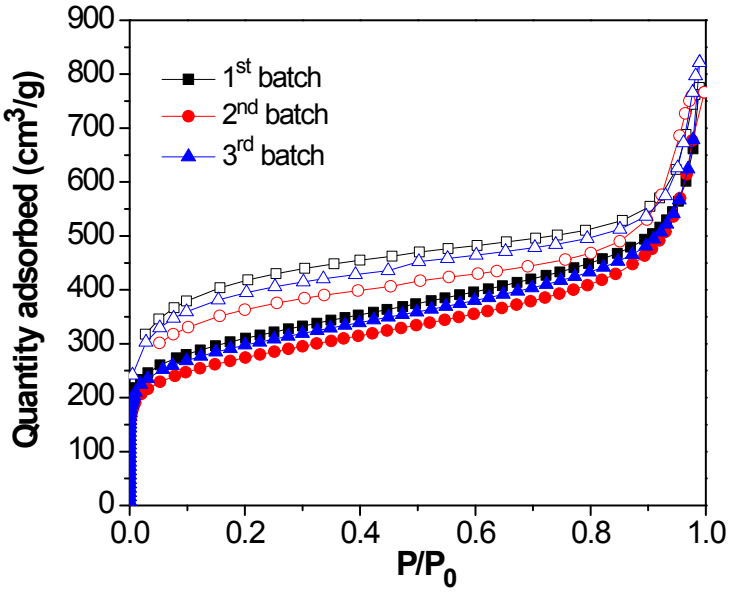

Figure S8. Nitrogen adsorption (filled symbols) and desorption (open symbols) isotherms for CP-CMP4 produced from different batch.

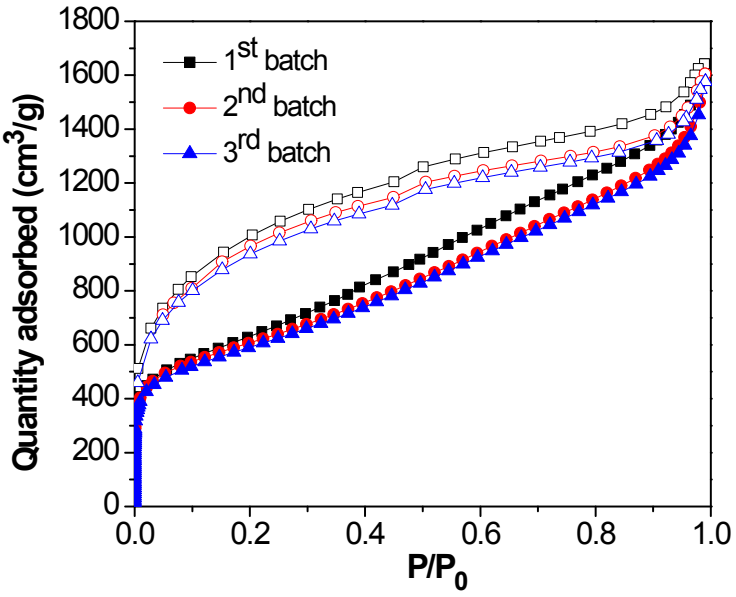

Figure S9. Nitrogen adsorption (filled symbols) and desorption (open symbols) isotherms for CP-CMP5 produced from different batch.

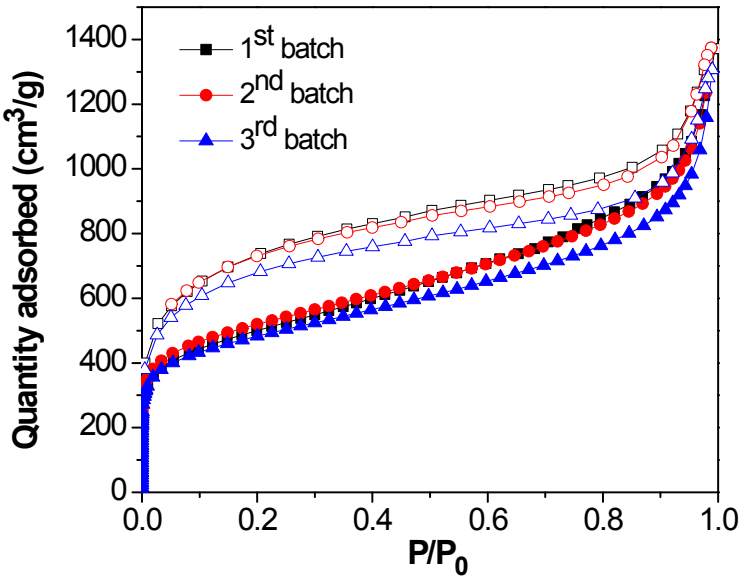

Figure S10. Nitrogen adsorption (filled symbols) and desorption (open symbols) isotherms for CP-CMP6 produced from different batch.

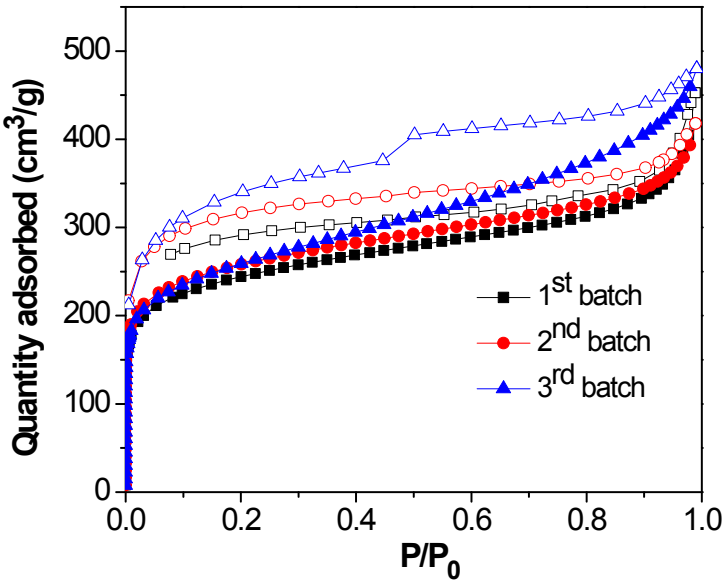

Figure S11. Nitrogen adsorption (filled symbols) and desorption (open symbols) isotherms for CP-CMP7 produced from different batch.

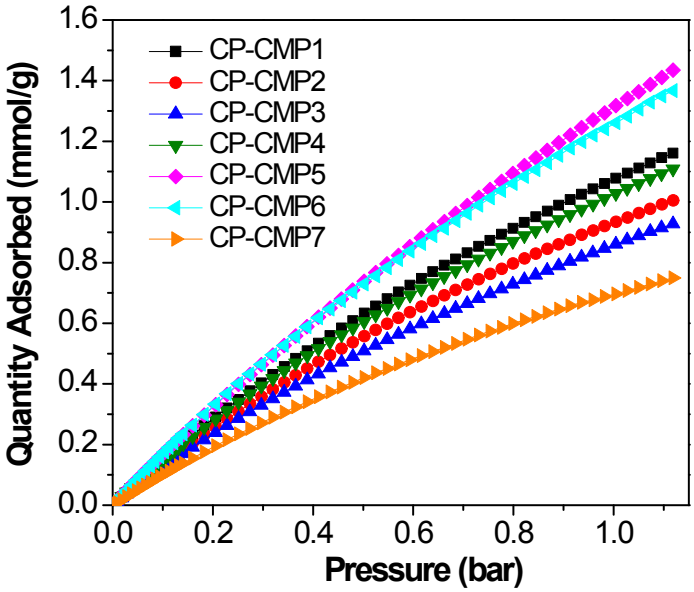

Figure S12. CH_4 adsorption isotherms for the copolymer networks collected at 273 K.

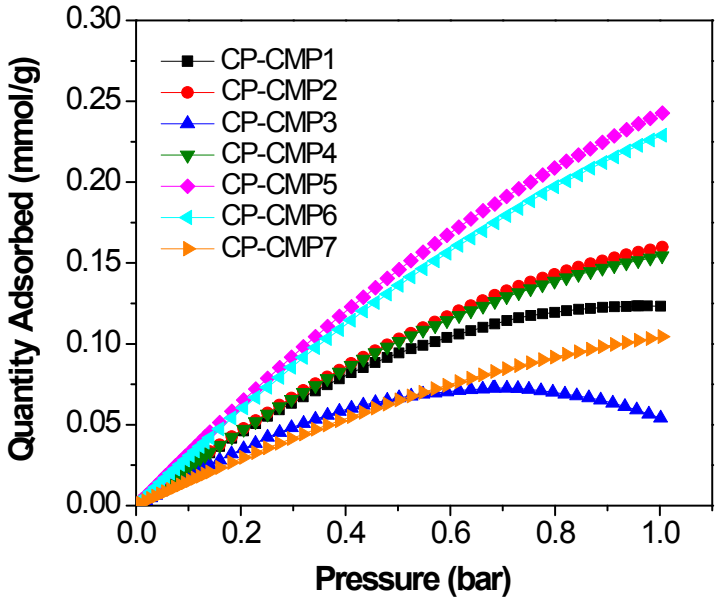

Figure S13. N_2 adsorption isotherms for the copolymer networks collected at 273 K.

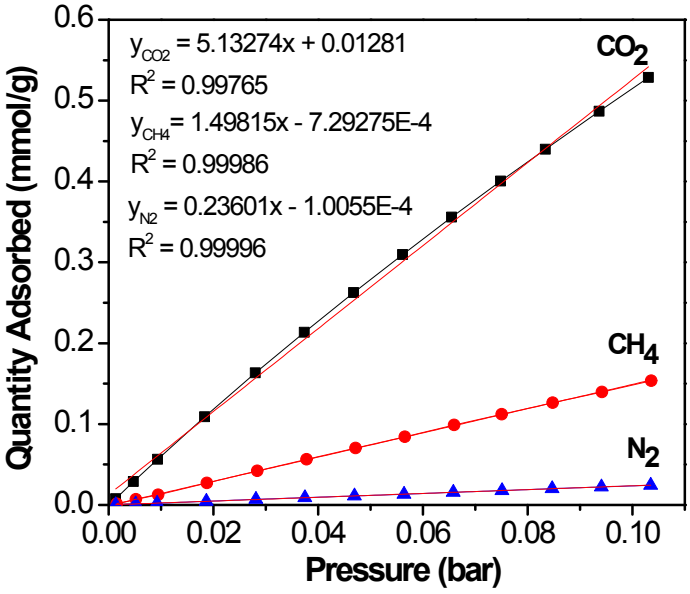

Figure S14. Gas adsorption selectivity for CP-CMP1 using the ratios of the Henry's law constant calculated from the initial slopes of the single-component gas adsorption isotherms collected at low pressure coverage (< 0.15 bar) and 273 K.

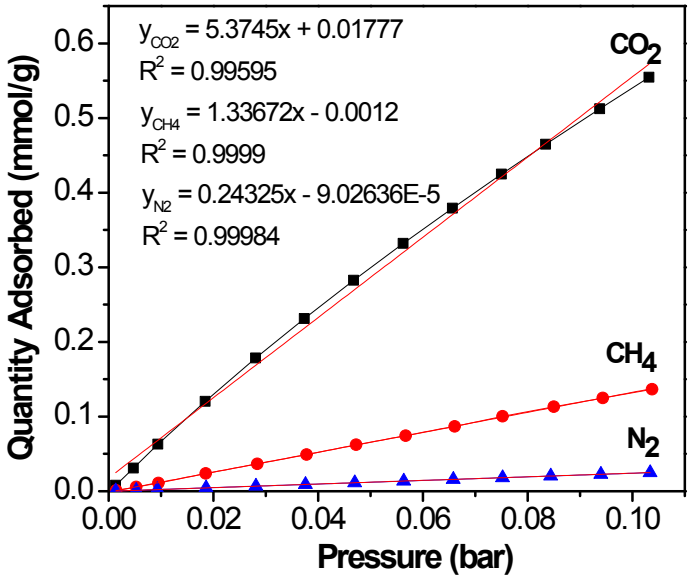

Figure S15. Gas adsorption selectivity for the CP-CMP2 using the ratios of the Henry's law constant calculated from the initial slopes of the single-component gas adsorption isotherms collected at low pressure coverage (< 0.15 bar) and 273 K.

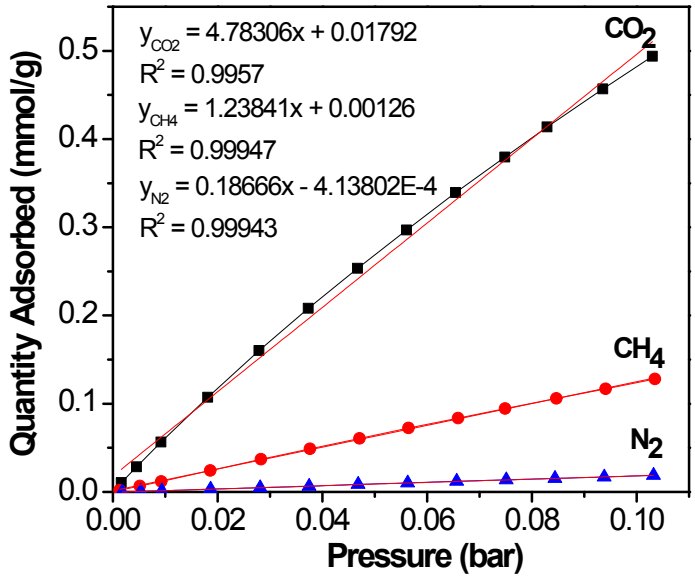

Figure S16. Gas adsorption selectivity for the CP-CMP3 using the ratios of the Henry's law constant calculated from the initial slopes of the single-component gas adsorption isotherms collected at low pressure coverage (< 0.15 bar) and 273 K.

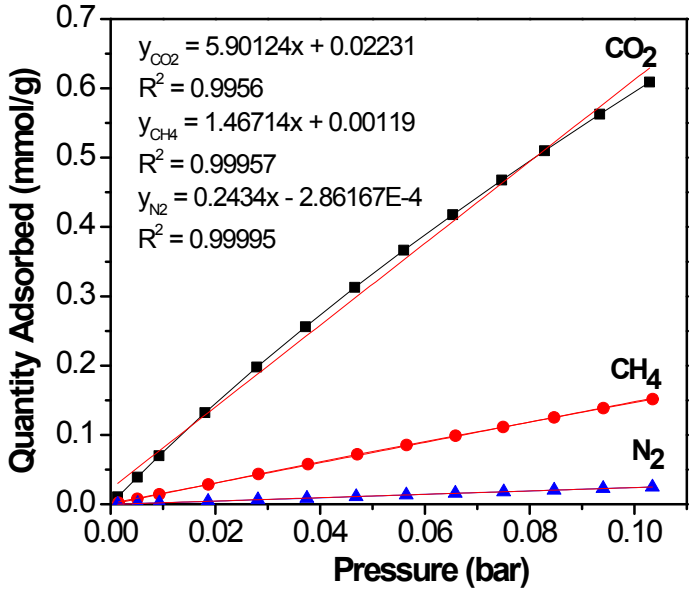

Figure S17. Gas adsorption selectivity for the CP-CMP4 using the ratios of the Henry's law constant calculated from the initial slopes of the single-component gas adsorption isotherms collected at low pressure coverage (< 0.15 bar) and 273 K.

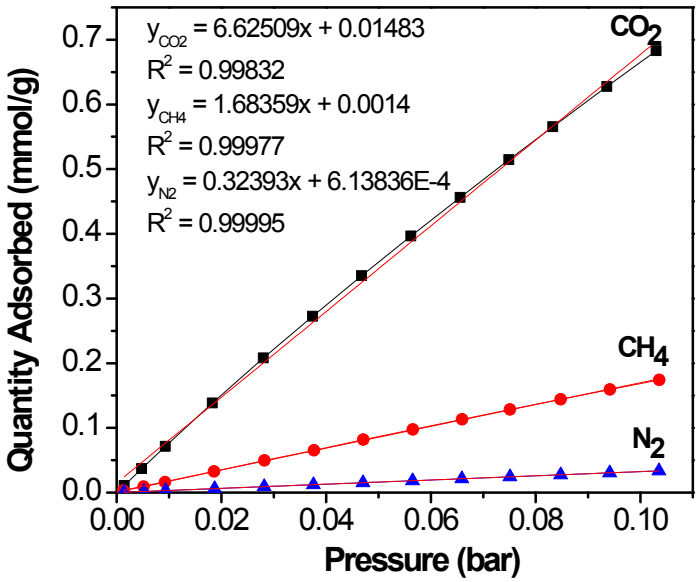

Figure S18. Gas adsorption selectivity for the CP-CMP5 using the ratios of the Henry's law constant calculated from the initial slopes of the single-component gas adsorption isotherms collected at low pressure coverage (< 0.15 bar) and 273 K.

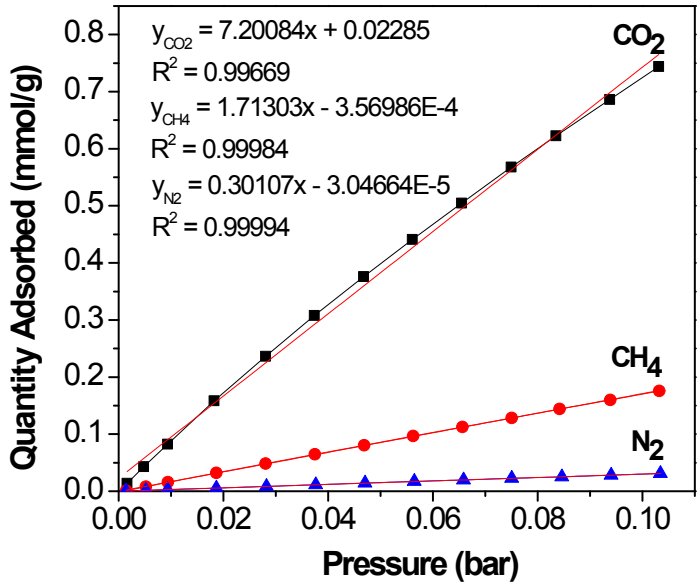

Figure S19. Gas adsorption selectivity for the CP-CMP6 using the ratios of the Henry's law constant calculated from the initial slopes of the single-component gas adsorption isotherms collected at low pressure coverage (< 0.15 bar) and 273 K.

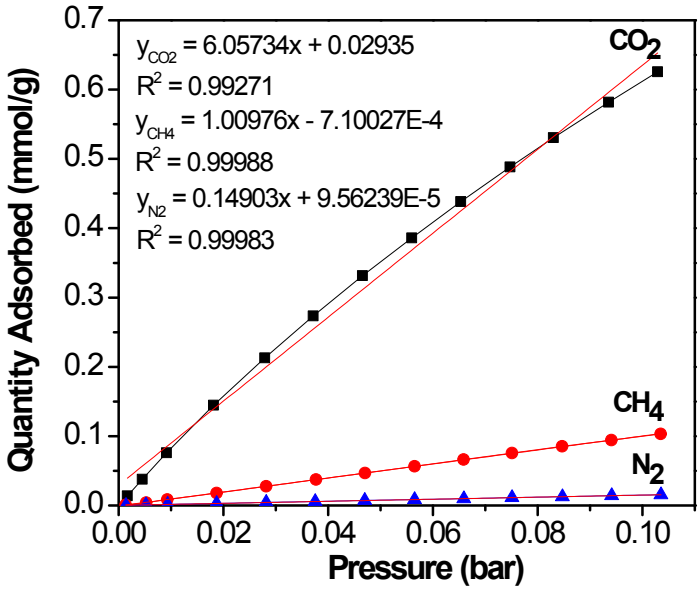

Figure S20. Gas adsorption selectivity for the CP-CMP7 using the ratios of the Henry's law constant calculated from the initial slopes of the single-component gas adsorption isotherms collected at low pressure coverage (< 0.15 bar) and 273 K.